Princeton Plasma Physics Laboratory

PPPL-5217

Effects of energetic particle phase space modifications by instabilities on integrated modeling

M. Podesta, M. Gorelenkova, E. Fredrickson, N. N. Gorelenkov, R. B.White

January 2016

Prepared for the U.S. Department of Energy under Contract DE-AC02-09CH11466.

Effects of energetic particle phase space modifications by instabilities on integrated modeling

M. Podestà[1], M. Gorelenkova[1], E. Fredrickson[1], N. N. Gorelenkov[1], R. B. White[1]

[1] Princeton Plasma Physics Laboratory, Princeton NJ 08543 - USA

E-mail: `mpodesta@pppl.gov`

Abstract.

Tokamak plasmas can feature a large population of energetic particles (EP) from Neutral Beam injection or fusion reactions. In turn, energetic particles can drive instabilities, which affect the driving EP population leading to a distortion of the original EP distribution function and of quantities that depend on it. The latter include, for example, Neutral Beam (NB) current drive and plasma heating through EP thermalization. Those effects must be taken into account to enable reliable and quantitative simulations of discharges for present devices as well as predictions for future burning plasmas. Reduced models for EP transport are emerging as an effective tool for long time-scale integrated simulations of tokamak plasmas, possibly including the effects of instabilities on EP dynamics. Available models differ in how EP distribution properties are modified by instabilities, e.g. in terms of gradients in real or phase space. It is therefore crucial to assess to what extent different assumptions in the transport models affect predicted quantities such as EP profile, energy distribution, NB driven current and energy/momentum transfer to the thermal populations. A newly developed *kick model*, which includes modifications of the EP distribution by instabilities in both real and velocity space, is used in this work to investigate these issues. Coupled to TRANSP simulations, the kick model is used to analyze NB-heated NSTX and DIII-D discharges featuring unstable Alfvén eigenmodes (AEs). Results show that instabilities can strongly affect the EP distribution function, and modifications propagate to macroscopic quantities such as NB-driven current profile and NB power transferred to the thermal plasma species. Those important aspects are only qualitatively captured by simpler fast ion transport models that are based on radial diffusion of energetic ions only.

PACS numbers: 52.50.Fa, 52.25.Fi, 52.55.Wq

1. Introduction

Enhanced fast ion transport caused by instabilities can be detrimental for the operation of fusion devices such as ITER and a Fusion Nuclear Science Facility [1]. Increased fast ion redistribution and losses reduce the fusion efficiency, affect the controllability and predictability of quantities such as Neutral Beam (NB) driven current and may cause harm to in-vessel structures. It is therefore important to develop and validate modeling tools that enable accurate predictions of fast ion transport in future devices, including the effects of plasma instabilities.

In this work, the TRANSP [2][3] tokamak transport code is used for integrated simulations of discharges from the NSTX spherical torus [4] and the DIII-D tokamak [5]. The main goal is to investigate whether - and for which quantities - a detailed modeling of the fast ion distribution function is required to obtain quantitatively meaningful results even when MHD instabilities are destabilized. It is anticipated that simple, *ad-hoc* diffusive models can already capture global features that are good indicators of a discharge performance, such as neutron rate, stored energy and overall NB current drive efficiency. However, a more rigorous treatment of the fast ion distribution evolution appears to be required to account for radial and temporal variations of integrals of the fast ion distribution. Examples include modeling of the NB driven current profile and contribution to the local power balance from the thermalizing fast ions.

The remainder of the paper is organized as follows. The modeling tools used in this work are introduced in Sec. 2, followed by a description of the target NSTX and DIII-D scenarios in Sec. 3. The main results of this study are then described in Sec. 4. Section 5 concludes the paper with a discussion of the main findings and their implications for future research.

2. Modeling tools and analysis procedure

The main numerical tool used for the whole-discharge integrated simulations considered herein is the tokamak transport code TRANSP [2][3]. Input profiles from the experiments include electron/ion density/temperature, q-profile, plasma toroidal rotation and magnetic equilibrium from the EFIT code [6]. Other quantities are constrained based on experimental measurements, such as total plasma current, surface voltage and NB injection parameters (active sources, geometry, injected power and current).

The NUBEAM module implemented in TRANSP models the fast ion evolution based on classical fast ion physics [7][8]. Several options are available in NUBEAM to account for fast ion transport mechanisms other than classical. Commonly used transport models are based on *ad-hoc* diffusivity and convection coefficients, which result in radial fast ion transport proportional to the local fast ion density gradient and density. In addition to the ad-hoc models, a physics-based reduced model (*kick model* [9]) has been recently implemented in TRANSP [10]. Contrary to the ad-hoc models of NUBEAM, the *kick model* accounts for the interaction of fast ions with instabilities in phase space, here represented through energy, canonical toroidal momentum and magnetic moment (E, P_ζ and μ respectively) following Ref. [11]. The model is based on a transport probability $p(\Delta E, \Delta P_\zeta|E, P_\zeta, \mu)$ associated to regions of phase space identified by E, P_ζ, μ. The probability describes changes (or *kicks*) in particle's energy and toroidal canonical momentum, ΔE and ΔP_ζ, resulting from fast ion interaction with instabilities [9]. The transport matrix is computed through particle-following codes such as ORBIT [12]. Perturbations used in ORBIT are modeled by MHD codes such as NOVA [13][14][15] that reproduce experimentally observed instabilities in terms of frequency and mode number spectrum. After an initial verification against the ORBIT code [9], the new model is now being tested against NSTX and DIII-D data [16][17]. Initial results compare well with experimental results and with predictions from a *critical gradient* model [18].

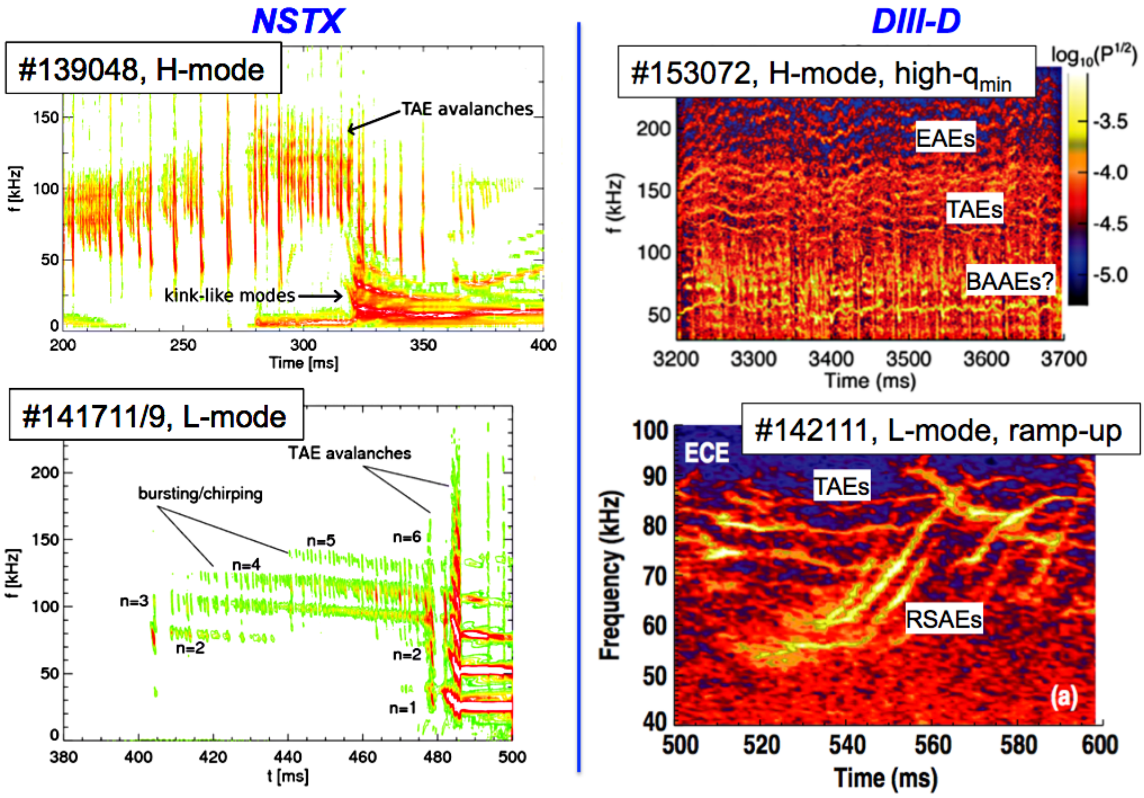

Figure 1. Frequency spectra as a function of time for the discharges investigated herein. Data are from pickup Mirnov coils located at the vessel wall for NSTX and from CO2 reflectometer data for DIII-D.

Device	*Shot no.*	B_0 *[T],* I_p *[MA]*	Confinement	*Instabilities*	*References*
NSTX	139048	0.45, 0.9	H-mode	RSAEs, TAEs, kink	[19] [20] [9] [10]
NSTX	141711, 141719	0.5, 0.9	L-mode	TAEs, kink	[21] [22] [23] [24]
DIII-D	142111	2.0, ramp-up	L-mode	RSAEs, TAEs	[25] [26] [27] [28]
DIII-D	153072	1.8, 2	H-mode	TAEs, EAEs, low-f AEs, NTM	[29] [30]

Table 1. Summary of NSTX and DIII-D discharges analyzed in this work. More details on each discharge are given in the References (last column).

3. Experimental scenarios

The discharges analyzed in this study have been selected to encompass a variety of NB-heated plasma scenarios, including L- and H-mode plasmas, ramp-up scenarios and high-q_{min}, nearly steady-state discharges (Fig. 1). All discharges feature robust Alfvénic activity. Dominant modes are identified as toroidal and reverse-shear Alfvèn eigenmodes (TAEs and RSAEs) based on their frequency, frequency evolution and mode structure. The latter is computed through the ideal MHD code NOVA, matching the measured frequency and (toroidal) mode numbers. (Details on the NOVA analysis can be found in Ref. [19]). Other instabilities such as kink-like modes and tearing modes, are present in some cases. DIII-D discharges also feature elliptical AEs at higher frequency than TAEs and RSAEs (see, for example, the spectrum for DIII-D discharge #153072 in Fig. 1).

For each discharge, three TRANSP runs are performed to compile a database with relevant quantities such as neutron rate, stored energy, NB driven current and fast ion density. The three runs refer to

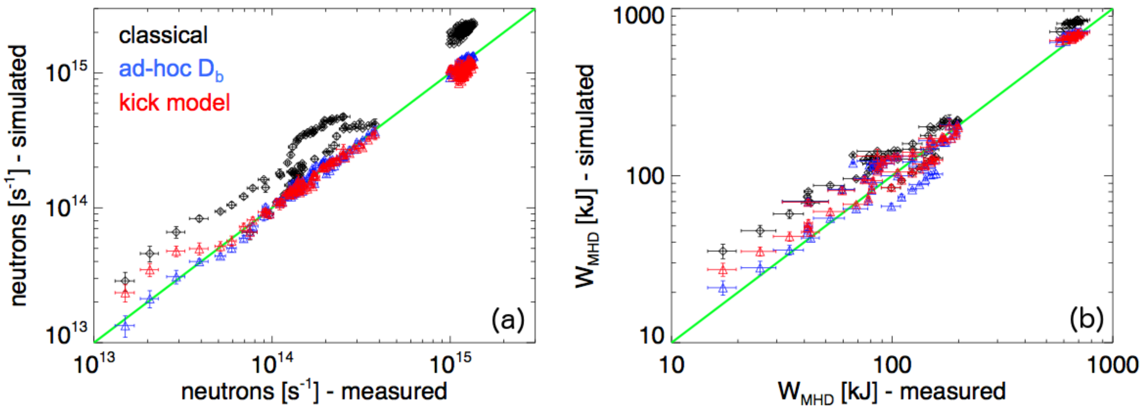

Figure 2. Comparison of (a) neutron rate and (b) stored energy computed by TRANSP against experimental values. Simulations are run with different assumptions for fast ion transport (classical physics; ad-hoc diffusion; kick model).

classical analysis, i.e. without any additional fast ion transport included; analysis with a time-dependent, spatially uniform fast ion diffusivity (called *ad-hoc model* in the following and in the figures); analysis with the phase space resolved *kick model* to simulate fast ion transport. The database is obtained by binning the quantities of interest (e.g. neutron rate, NB driven current, NB ion density) every 10 ms. Error bars shown in the figures refer to the standard deviation of the different quantities within the 10 ms time window. Error bars do not include possible systematic errors from the experimental measurements.

For the ad-hoc model, the diffusivity D_b is adjusted as a function of time to match the measured neutron rate and stored energy (W_{MHD}, reconstructed through the EFIT code for equilibrium reconstruction [6]), cf. Fig. 2. A similar procedure is here adopted to adjust the amplitude scaling factor for each mode included in the kick model. Starting from the experimental mode amplitude (when available), corrections are applied iteratively to optimize the match with neutron rate and W_{MHD}. Results of this procedure are also shown in Fig. 2, which compares the measured neutron rate and W_{MHD} with the results for the three TRANSP runs for all discharges in the database.

Not surprisingly, *classical* runs over-estimate both neutron rate and stored energy with respect to the experiments. That indicates that classical runs over-predict the fast ion content in the plasma. In the experiments, fast ion transport is enhanced by instabilities, resulting in decreased fast ion confinement and therefore lower neutron rate and stored energy. Note that, since thermal plasma profiles are given as input, changes in the total W_{MHD} are caused by fast ion transport only. Overall, both the *ad-hoc* and *kick* models are capable to recover the drop in the measured quantities within the experimental uncertainties, as illustrated in Fig. 2. The next Sections assess the resulting changes in other important quantities that are usually derived through integrated simulations.

4. Results from combined NSTX and DIII-D database

A first result from the combined NSTX/DIII-D analysis is presented in Fig. 3. The NB current drive efficiency with respect to classical simulations is shown as a function of the inferred deficit in neutron rate, defined as the relative departure of computed neutron rate from predictions assuming classical

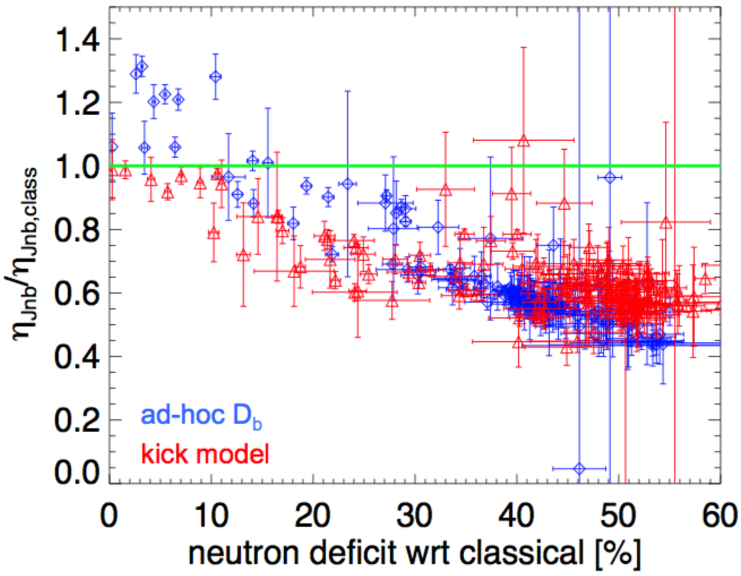

Figure 3. NB current drive efficiency, normalized to the *classical* case, as a function of the measured deficit in neutron rate with respect to classical simulations. Results from the two fast ion transport model (ad-hoc diffusivity and kick model) are shown.

fast ion behavior. Since the deficit is roughly proportional to the amount of Alfvénic activity (see, for instance, Figs. 8-10 in Ref. [29]), the abscissa in Fig. 3 can be taken as an indicator of the severity of the instabilities. NB current drive efficiency is here defined as the ratio of NB driven current to the total current, normalized to the injected NB power.

For the cases considered herein, up to 60% neutron rate deficit is observed. The corresponding reduction of NB current drive efficiency is $20-60\%$. This large reduction indicates that these effects must certainly be taken into account for accurate, quantitative modeling and interpretation of the experimental data. From Fig. 3, differences are observed in the values predicted by using either the *ad-hoc* diffusion or the kick model to account for enhanced fast ion transport by instabilities. This suggests that a correct treatment of the fast ion evolution is required, possibly including phase space effects when resonant instabilities are observed.

4.1. Modifications of the fast ion distribution function

A critical indicator of the effects of instabilities on the fast ion population is provided by the fast ion distribution function, here computed by the NUBEAM module of TRANSP. Figure 3 shows an example from a NSTX discharge with unstable TAEs that develop into so-called avalanches, i.e. large amplitude bursts of the modes followed by drops in the measured neutron rate and enhanced losses. Effects of the instabilities are clearly not taken into account in the classical TRANSP run, which is taken as reference for the analysis with the two other transport models.

Consistently with the decrease in neutron rate and stored energy, additional fast ion transport causes a reduction in the core fast ion content. Significant differences are observed when the simple diffusive model or the kick model are used, see Fig. 4 for an example from NSTX discharge #139048. When

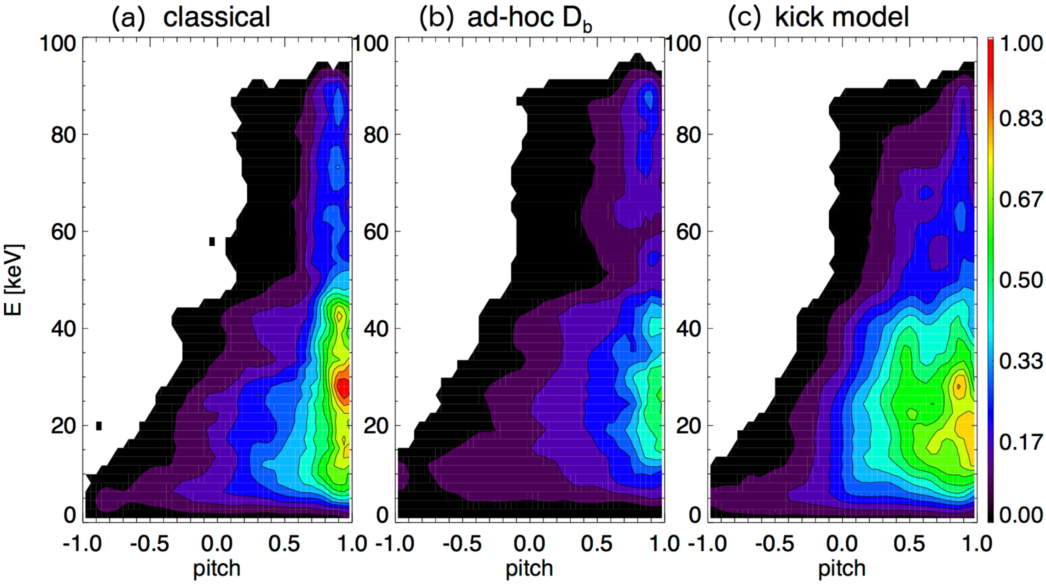

Figure 4. Example of fast ion distribution functions as a function of energy and pitch (ratio of parallel to total velocity) under different assumptions for fast ion transport mechanisms: (a) classical, (b) ad-hoc diffusion, (c) kick model. Note the broadening of the distribution in panel (c), resulting from particles with large pitch being pushed to smaller pitch values by instabilities.

uniform radial diffusion is applied, the entire distribution is reduced by a similar amount, regardless of the energy or pitch of the fast particles. For the kick model, however, some regions of the distribution suffer a larger depletion than others. More specifically, for the dominant TAE/RSAEs present in the selected discharges, higher energy co-passing particles are transported more efficiently. This is consistent with the fact that co-passing particles are the ones resonating more efficiently with the instabilities, and therefore are more prone to be affected by the modes. As a consequence, particles are pushed to smaller pitch (cf. Fig. 4c), resulting in broader distributions and a larger population of barely passing or trapped particles. More details on modeling results for the distribution function can be found elsewhere [31]. These observations can be expected to imply differences for other quantities that result from integrals of the fast ion distribution over phase space variables.

4.2. Radial profiles

Experimentally, Alfvénic instabilities are known to cause flattening and reduction in the beam ion density, n_b (see, for example, Ref. [32]). Information on the radial profile of the NB driven current is much more difficult to obtain directly from the experiments, and analysis through codes such as TRANSP is required. Figure 5 shows a comparison of the peaking factor computed for the NB driven current, J_{NB}, based on the three assumptions for fast ion transport. The peaking is computed as the ratio between central current to its average over the entire minor radius.

As a general result from the NSTX/DIII-D database, the peaking is reduced by up to a factor 2 with respect to *classical* simulations without additional fast ion transport, indicating a net redistribution of current towards larger minor radii. On average, the two transport models predict a comparable broadening of the J_{NB} profile. However, as expected from the differences observed in the fast ion

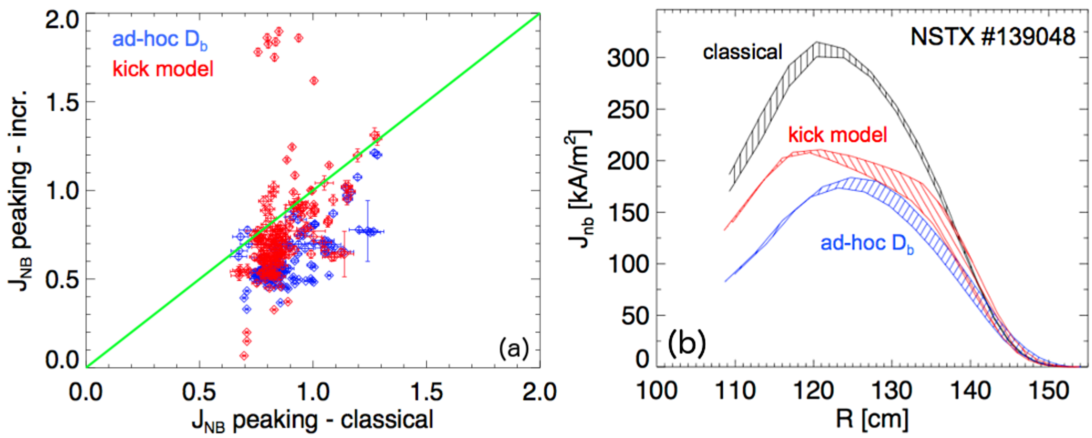

Figure 5. (a) Comparison of NB-driven current peaking factor from runs using ad-hoc diffusion or kick model with respect to classical simulations. Overall, enhanced fast ion transport results in a decrease in current peaking, i.e. broader NB-driven current profiles. (b) Although average quantities such as the peaking factor are similar, the radial profiles of J_{NB} can differ substantially between the two models.

distribution function, the radial profiles of the NB-driven current obtained with the two models can be quite different (Fig. 5b). This results from the phase space selectivity of the kick model, not present in the ad-hoc model.

Implications are not limited to the non-inductive current profile. Since the total current is imposed in these analyses, variations of $J_{NB}(r)$ automatically imply changes in the ohmic current profile as well. The bootstrap current is not affected, since thermal plasma profiles are given as input in the simulations. Different ohmic current profiles, in turn, result in changes in the ohmic heating, which can be a significant source term for the overall (local) power balance. (Incidentally, it is noted that even larger variations in the predicted quantities can be expected for *predictive* simulations, for which total current, q-profile and magnetic configuration may not be imposed as input but computed self-consistently).

Further differences in the TRANSP results are observed from a combined analysis of the evolution of fast ion density and NB driven current profiles, see Fig. 6. A broadening is predicted in both quantities, with significant reduction of the fast ion density peaking with respect to classical simulations. An important difference for the two transport models is the correlation between J_{NB} and fast ion density evolution that results from the kick model. Figure 6b shows an example from a high-q_{min}, nearly steady-state DIII-D discharge, for which J_{NB} and n_b peaking computed with the kick model align along a (roughly) straight line. This correlation is not found in simulations based on either classical or ad-hoc diffusive transport hypotheses. More analysis is required to assess the generality of these results. However, they suggest that the correlation between energy and canonical angular momentum changes induced by resonant instabilities [11], which is included in the kick model, can also propagate to integrated quantities. Since current is proportional to parallel velocity, $\propto \sqrt{E}$, and $P_\zeta \propto \Psi$, this establishes a correlation between J_{NB} and n_b modifications.

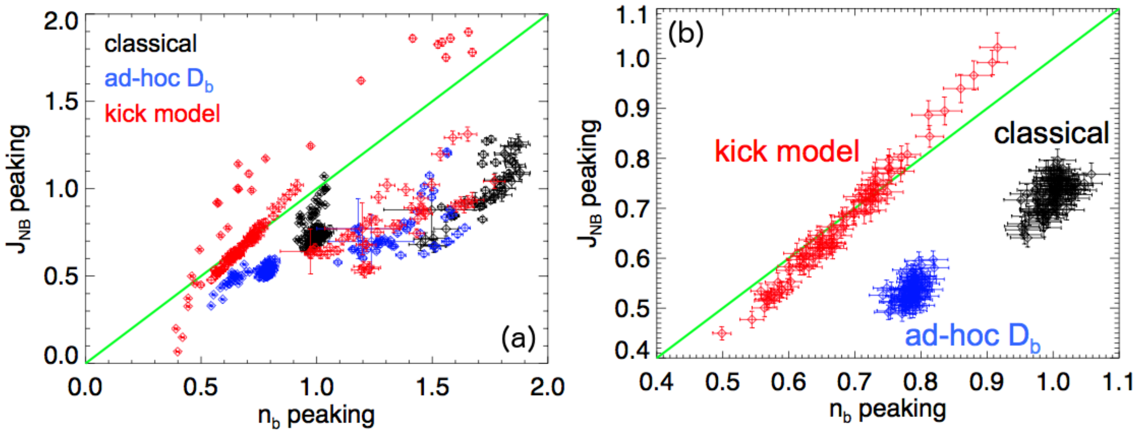

Figure 6. (a) Peaking of NB driven current with respect to peaking of NB ion density. Colors refer to classical simulations (black) and to runs using ad-hoc diffusivity (blue) or the kick model (red) to account for enhanced NB ion transport. (b) Detail from panel (a) for DIII-D discharge #153072, showing the correlation between J_{NB} and n_b profiles that can result from the kick model.

4.3. Power balance

As a final example of the effects of fast ion modeling on results from integrated simulations, Fig. 7a shows the computed power transferred through thermalization from the slowing-down NB ions to the thermal electron population for the same database presented above. When additional fast ion transport is included in the simulations, a reduction of up to ~ 2 in the power with respect to *classical* simulations is computed. A similar reduction is observed in the power flowing from NB ions to thermal ions (not shown in the figure). Similarly to the results for NB driven current profiles, the overall reduction is comparable for the two transport models compared here, but the radial profiles can be substantially different as shown in Fig. 7b for NSTX discharge #139048.

As mentioned in Sec. 4.2, other heat source terms, such as the ohmic current profile, are also modified depending on the NB ion transport model adopted. This potentially large difference in source terms can lead to profound differences in a power balance analysis, e.g. to estimate the local thermal diffusivities. In general, the use of different fast ion transport models has more ramifications than it could appear at a first glance. One advantage of implementing improved fast ion transport models in codes such as TRANSP is that those secondary effects and multiple feedback loops can be taken into account consistently.

5. Conclusions

Integrated simulations of tokamak discharges based on classical fast ion physics have been compared to simulations including enhanced fast ion transport by plasma instabilities through two different models implemented in the TRANSP code. The key difference between the two models is whether fast ion transport is limited to a simple radial diffusion or it includes phase space modifications. A database from NSTX and DIII-D discharges featuring robust MHD activity has been selected to assess the generality of the results.

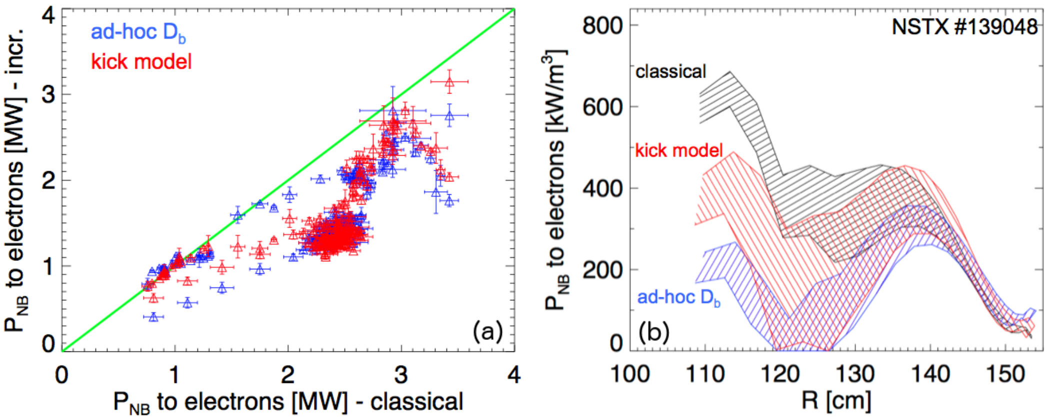

Figure 7. (a) Comparison of NB power flowing to thermal electrons from classical simulations and from runs using ad-hoc diffusivity (blue) or the kick model (red). (b) Radial profiles of NB power to electrons for NSTX discharge #139048 around 300 ms.

The two transport models generally lead to similar predictions for global quantities such as neutron rate, stored energy and NB current drive efficiency. (In fact, the first two quantities are often used to calibrate the free parameters of the models). This justifies the use of the simpler *ad-hoc* diffusive model for routine analysis, e.g. to compare discharges in terms of overall performance (see, for example, Refs [33][34][35][36][37]). It also confirms the validity of recent upgrades to the simple diffusive model in TRANSP, which now accepts a target neutron rate waveform as input and adjusts the diffusion coefficient during the run to match the input [38]. The latter feature is certainly useful for rapid analysis, e.g. during an experimental session when time for in-between-shots analysis is limited.

The main differences between the two models arise in the radial profiles of quantities resulting from integrals of the fast ion distribution function. A first reason for this is that a spatially uniform diffusivity has been used herein for the *ad-hoc* model. In principle, a radial dependence $D_b(r)$ can be provided as input to TRANSP. However, there are no rigorous criteria to select a specific radial profile for an ad-hoc parameter such as D_b. On the contrary, the radial dependence (through the P_ζ phase space variable) is implicit in the kick model probabilities, which are computed based on the radial mode structure of the observed instabilities.

A second reason for different results from the two models is the possible correlation between energy and P_ζ variations, resulting from the resonant nature of the wave-particle interaction [11], which is included in the kick model. That same relationship can also lead to important correlations between different quantities and their temporal evolution, for example between NB driven current profile and beam ion density, that are not reproducible by the simple diffusive model.

As a first step, this work has focused on the analysis of discharges from existing devices. It can be expected that discrepancies in the results based on the different fast ion transport models can be further amplified when the TRANSP code is used in *predictive* mode. In that case, the reduced number of constraints translates in an increased number of unknowns in the simulation, which must be computed self-consistently. Exploration of the potential of the kick model for more consistent predictive runs when MHD instabilities are expected to be destabilized will be the subject of future work.

Acknowledgments

Contributions from - and useful discussions with - the NSTX-U and DIII-D Energetic Particles groups is kindly acknowledged. This work was supported by the US DOE Office of Science (Office of Basic Energy Sciences) under Contract Number DE-AC02-09CH11466. NSTX-U at Princeton Plasma Physics Laboratory (Princeton University, New Jersey - USA) is a DOE Office of Science User Facility. The digital data for this paper can be found in http://arks.princeton.edu/ark:/88435/dsp018p58pg29j

[1] FASOLI, A. et al., Nucl. Fusion **47** (2007) S264.

[2] HAWRYLUK, R., An empirical approach to tokamak transport, in Physics of plasmas close to thermonuclear conditions, Proceedings from the International School of Plasma Physics, 1979, Villa Monastero, Varenna - Italy, 1979.

[3] More details on the TRANSP code available at http://w3.pppl.gov/˜pshare/help/transp.htm.

[4] ONO, M. et al., Nucl. Fusion **40** (2000) 557.

[5] LUXON, J. L., Fusion Sci. Technol. **48** (1985) 828.

[6] LAO, L. L. et al., Nucl. Fusion **25** (1985) 1611.

[7] PANKIN, A. et al., Computer Physics Communication **159** (2004) 157.

[8] GOLDSTON, R. J. et al., J. Comput. Phys. **43** (1981) 61.

[9] PODESTà, M. et al., Plasma Phys. Control. Fusion **56** (2014) 055003.

[10] PODESTà, M. et al., Nucl. Fusion **55** (2015) 053018.

[11] WHITE, R. B., The theory of toroidally confined plasmas, Imperial College Press, London, UK, 3nd edition, 2014.

[12] WHITE, R. B. et al., Phys. Fluids **27** (1984) 2455.

[13] CHENG, C. Z., Phys. Rep. 211 **1** (1992).

[14] FU, G. Y. et al., Stability of the toroidicity-induced Alfvén eigenmode in axysimmetric toroidal equilibria, Phys. Fluids B **5** (1993) 4040.

[15] GORELENKOV, N. N. et al., Phys. Plasmas **6** (1999) 2802.

[16] PODESTà, M. et al., Effects of fast ion phase space modifications by instabilities on fast ion modeling, in 14th IAEA Technical Meeting on Energetic Particles in magnetic confinement systems, O-01, Vienna, Austria, 2015.

[17] KRAMER, G. J., in preparation (2015).

[18] GORELENKOV, N. N. et al., Validating predictive models for fast ion profile relaxation in burning plasmas, in 14th IAEA Technical Meeting on Energetic Particles in magnetic confinement systems, O-06, Vienna, Austria, 2015.

[19] FREDRICKSON, E. D. et al., Phys. Plasmas **16** (2009) 122505.

[20] FREDRICKSON, E. D. et al., Nucl. Fusion **53** (2013) 013006.

[21] PODESTà, M. et al., Nucl. Fusion **52** (2012) 094001.

[22] DARROW, D. S. et al., Plasma and Fusion Research (submitted, 2012).

[23] DARROW, D. S. et al., Stochastic orbit loss of neutral beam ions from NSTX due to toroidal Alfvén eigenmode avalanches, Nucl. Fusion **53** (2013) 013009.

[24] LIU, D. et al., Phys. Plasmas **22** (2015) 042509.

[25] Van Zeeland, M. A. et al., Phys. Plasmas **18** (2011) 056114.

[26] SPONG, D. A. et al., Phys. Plasmas **19** (2012) 082511.

[27] SPONG, D. A., Nucl. Fusion **53** (2013) 053008.

[28] TODO, Y. et al., Nucl. Fusion **55** (2015) 073020.

[29] HEIDBRINK, W. W. et al., Plasma Phys. Control. Fusion **56** (2014) 095030.

[30] HOLCOMB, C. T. et al., Phys. Plasmas **22** (2015) 055904.

[31] PODESTà, M. et al., Phys. Plasmas (submitted, 2015).

[32] HEIDBRINK, W. W. et al., Phys. Rev. Lett. **99** (2007) 245002.

[33] BARANOV, Y. F. et al., Plasma Phys. Control. Fusion **51** (2009) 044004.

[34] GERHARDT, S. P. et al., Nucl. Fusion **51** (2011) 033004.

[35] TURNYANSKIY, M. et al., Nucl. Fusion **53** (2013) 053016.

[36] HEIDBRINK, W. W. et al., Plasma Phys. Control. Fusion **56** (2014) 095030.

[37] KLIMEK, I. et al., Nucl. Fusion **55** (2015) 023003.

[38] KAYE, S. M., 2015, private communication.

Princeton Plasma Physics Laboratory
Office of Reports and Publications

Managed by
Princeton University

under contract with the
U.S. Department of Energy
(DE-AC02-09CH11466)

P.O. Box 451, Princeton, NJ 08543
Phone: 609-243-2245
Fax: 609-243-2751

E-mail: publications@pppl.gov

Website: http://www.pppl.gov